Dalton Transactions

PAPER

Cite this: *Dalton Trans.*, 2014, **43**, 11739

Ferrocene analogues of sandwich $M(CrB_6H_6)_2$: a theoretical investigation†

Lifen Li, Chang Xu, Baokang Jin and Longjiu Cheng*

Received 14th April 2014,
Accepted 9th June 2014

DOI: 10.1039/c4dt01106f

www.rsc.org/dalton

The stability and electronic structures of the new sandwich compounds $M(CrB_6H_6)_2$ ($M = Cr, Mn^+, Fe^{2+}$) are investigated by density functional theory. All the investigated sandwich complexes are in D_{6d} symmetry and all of them are thermodynamically stable according to the large HOMO–LUMO gap, binding energy, vertical ionization potential and vertical electron affinity analyses, as well as $Fe(C_5H_5)_2$ and $Cr(C_6H_6)_2$, following the 18-electron principle. The natural bond orbital, detailed molecular orbitals and adaptive natural density partitioning analyses suggest that the spd–π interaction plays an important role in the sandwich compounds. This work challenges the traditional chemical bonding of the inorganic metal compound, investigates first the bonding style of the d atom orbital interacting with the π MO which was formed by p–d atomic orbitals, and indicates that the metal-doped borane ring can also be an ideal type π-electron donor ligand to stabilize the transition metal.

1. Introduction

Metallocenes have attracted much attention since the transition metal π-complex, ferrocene ($Fe(C_5H_5)_2$), was discovered in 1951.[1,2] Lots of organometallic compounds have been investigated experimentally and theoretically.[3–17] Warren[7] investigated the metal sandwich complexes by the charge transfer process and molecular orbitals. Clark *et al.*[8] studied the metal–ligand interaction in 3d sandwich complexes. Two typical sandwich clusters, $Fe(C_5H_5)_2$ [18–29] and $Cr(C_6H_6)_2$,[23,24,27,30–42] have been studied extensively. For $Fe(C_5H_5)_2$, the metal Fe atom contributes eight electrons ($3d^6 4s^2$) and each of the C atoms contributes one electron, which follows the 18-electron principle. Similarly, the Cr atom of $Cr(C_6H_6)_2$ contributes six electrons ($3d^5 4s^1$) and each of the 12 carbons contributes one electron, which also follows the 18-electron principle. With more studies on sandwich compounds, various ligands have been obtained. The ferrocene analogues $[(\eta^5\text{-}E_5)_2M]$ (E = P, N, As, Sb, and Bi) have found important applications in both fundamental research and materials science.[1,43–49] Besides, planar aromatic $[Al_4]^{2-}$,[50–54] $[N_5]^-$,[49] $[(P_5)_2Ti]^{2-}$,[55] borane,[56,57] CO,[58] PH_3,[58] and boron clusters[59–63] can also be utilized as ligands to coordinate transition metals and form similar $[(\eta^n\text{-}E_n)_2M]$ complexes (n = 4–6).

Recently, we have studied the chemical bonding and electron structure of $Cr@B_6H_6$ in C_{6v} symmetry, which features a Cr atom in a planar hexacoordinate environment at the center of a perfect B_6H_6 hexagon.[64] Inspired by the proposed 6-π electron aromatic $Cr@B_6H_6$, we present herein an investigation by density functional theory (DFT) of a new class of sandwich-type complexes, D_{6d} $M(CrB_6H_6)_2$ ($M = Cr, Mn^+, Fe^{2+}$). The compounds contain two parallel η^6-CrB_6H_6 hexagons with two nearly planar hexacoordinate Cr atoms located at the center along the sixfold molecular axis. These complexes are unique in that the delocalized π molecular orbitals (MOs) of the ligand, which interacted with the partially occupied d orbitals of the transition metal, possess the d orbital component of the Cr atom at the center of the planar B_6H_6 hexagon. To the best of our knowledge, there have been no investigations reporting the metal-doped borane ligands in sandwich-type complexes. The results obtained in this work provide an important extension to the traditional concept of metallocene-like complexes by incorporating hexacoordinate transition metal atoms into the systems.

2. Computational details

The geometries of $M(CrB_6H_6)_2$ ($M = Cr, Mn^+, Fe^{2+}$) are optimized using the TPSSh[65] functional. The optimization and the calculations of the energies and HOMO–LUMO gaps are performed at the TPSSh/6-311+G** level. We analyze the vibrational frequencies for checking the stability of structures at the same theoretical level. The TPSSh functional was proven to give reasonably accurate energetic properties of boron and boron-based clusters.[64,66–69] The binding energy of the

---

Department of Chemistry, Anhui University, Hefei, Anhui 230039, People's Republic of China. E-mail: clj@ustc.edu; Tel: +86-551-5107342

† Electronic supplementary information (ESI) available: Fig. S1 and S2 include the partial canonical molecular orbitals and AdNDP localized bonding patterns of $[Mn(CrB_6H_6)_2]^+$ and $[Fe(CrB_6H_6)_2]^{2+}$; the coordinates of $M(CrB_6H_6)_2$ ($M = Cr, Mn^+, Fe^{2+}$) (in angstroms). See DOI: 10.1039/c4dt01106f

compound is defined as $E_b = E(M(CrB_6H_6)_2) - E(M) - E(CrB_6H_6)$. Then, the vertical ionization potential (VIP) of $Cr(CrB_6H_6)_2$ is calculated as $E([Cr(CrB_6H_6)_2]^+) - E(Cr(CrB_6H_6)_2)$, the vertical electron affinity (VEA) of $Cr(CrB_6H_6)_2$ is $E(Cr(CrB_6H_6)_2) - E([Cr(CrB_6H_6)_2]^-)$, and VEA of $[Mn(CrB_6H_6)_2]^+$ is $E([Mn(CrB_6H_6)_2]^+) - E(Mn(CrB_6H_6)_2)$. Natural bond orbital (NBO) analyses and adaptive natural density partitioning (AdNDP) analyses are implemented to gain insight into the bonding pattern of the complexes. All calculations are carried out using the GAUSSIAN 09 package.[70]

3. Results and discussion

We optimize $M(CrB_6H_6)_2$ ($M = Cr, Mn^+, Fe^{2+}$) at the TPSSh/6-311+G** level. Fig. 1 depicts the optimized staggered configurations of $M(CrB_6H_6)_2$. The binding energy, energy gap, VEA, VIP, rotation energy of $M(CrB_6H_6)_2$, $Fe(C_5H_5)_2$ and $Cr(C_6H_6)_2$ are listed in Table 1, as well as the natural atomic charges of $M(CrB_6H_6)_2$.

3.1. Structural and chemical stability

The staggered configurations of $M(CrB_6H_6)_2$ sandwich structures are all found to be true local minima by frequency check. The difference among the bond lengths of $Cr(CrB_6H_6)_2$, $[Mn(CrB_6H_6)_2]^+$ and $[Fe(CrB_6H_6)_2]^{2+}$ is little as shown in Fig. 1. The lengths of the B–B bond and Cr–B bond in the ligands (1.81 Å and 1.90 Å, respectively) became longer after forming sandwich compounds (1.84–1.85 Å and 1.94 Å, respectively). The bond lengths of the M–Cr bonds are 2.14–2.16 Å, and of the M–B bonds are 2.39–2.43 Å. As a comparison, the M–C bond lengths in D_{5h} $Fe(C_5H_5)_2$ and D_{6h} $Cr(C_6H_6)_2$ are 2.04 Å and 2.14 Å as calculated at the same theoretical level.[77] Fig. 2 gives the energy of $Cr(CrB_6H_6)_2$, $Fe(C_5H_5)_2$ and $Cr(C_6H_6)_2$ in different angles, which vividly shows that the most stable configuration of $Cr(CrB_6H_6)_2$ is the staggered configuration and that of $Fe(C_5H_5)_2$ and $Cr(C_6H_6)_2$ is the eclipsed configuration. Although the energy differences between the staggered (D_{6d}) and the eclipsed (D_{6h}) conformations are very small (0.13–0.19 eV), the eclipsed $M(CrB_6H_6)_2$ complexes all turn out to be transition states with one imaginary located at 64i, 68i, and 69i cm^{-1}, respectively. When relaxed in the modes with the imaginary frequencies mentioned above, the eclipsed $M(CrB_6H_6)_2$ complexes are automatically transferred to the staggered conformation since the transition states are on rotational paths.

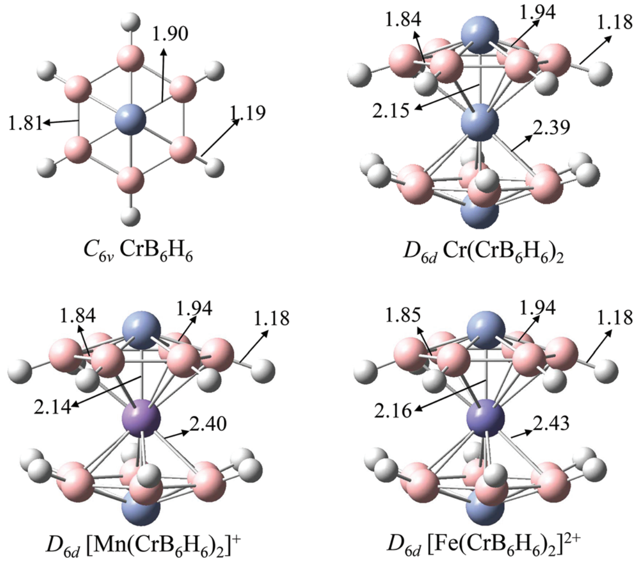

Fig. 1 The optimized structures of the ligand CrB_6H_6 and the sandwich $M(CrB_6H_6)_2$ for $M = Cr, Mn^+$ and Fe^{2+}. The symmetry and bond lengths are labeled in the figure; H – white, B – brown, Cr – stone blue, Mn – purple, Fe – royal purple.

The stability of these compounds is evaluated theoretically. The fairly large HOMO–LUMO energy gaps (1.77–2.31 eV) and the binding energy (3.03–13.92 eV) of $M(CrB_6H_6)_2$ suggest high stability of these systems. Besides, the VIP values (7.38 eV) of $Cr(CrB_6H_6)_2$ and the VEA values (6.87 eV) of the cation $[Mn(CrB_6H_6)_2]^+$ are similar to the VIP values of ferrocene (7.14 eV) and dibenzenechromium (5.40 eV), and the VEA value (2.81 eV) of $Cr(CrB_6H_6)_2$ is small but larger than the values of ferrocene (−0.34 eV) and dibenzenechromium (−0.27 eV), which indicates that the natural molecules of $Cr(CrB_6H_6)_2$ and the cations of $Mn(CrB_6H_6)_2$ are stable. Moreover, the Wiberg bond indices (WBIs)[71] reveal that the strength of the B–H and B–B bonds in CrB_6H_6 ligands is well maintained and that of the Cr–B bonds is decreased (0.99 in the ligand and 0.79–0.80 in the sandwich complexes), when the introduction of a transition metal center, M, leads to two additional Cr–M bonds and twelve additional B–M bonds. The calculated total WBIs of the constituent atoms with $WBI_H = 1.00$, $WBI_B = 3.31–3.43$, $WBI_{Cr} = 6.30–6.36$, and $WBI_M = 4.45–5.75$ indicate that the center metal atoms interact strongly with the ligands.

3.2. Aromaticity

The ligand CrB_6H_6 is a highly aromatic analogue of benzene, and we suggest that there may be delocalized electrons in $M(CrB_6H_6)_2$ as well as $Fe(C_5H_5)_2$ and $Cr(C_6H_6)_2$. Since delocali-

Table 1 Energy gap, ΔE_{HL} [eV]; binding energy, E_b [eV]; vertical ionization potential, VIP [eV]; vertical electron affinity, VEA [eV]; rotation energy, E_r [eV]; and natural atomic charges, q [|e|] for $M@(CrB_6H_6)_2$ ($M = Cr, Mn^+$) and $Cr@(C_6H_6)_2$ at the TPSSh/6-311+G** level

	ΔE_{HL}	E_b	VIP	VEA	E_r	q_{Cr}	q_B	q_M	q_H
$Cr@(CrB_6H_6)_2$	1.77	3.60	7.38	2.81	0.19	+0.38	−0.11	+0.67	−0.01
$[Mn@(CrB_6H_6)_2]^+$	2.31	3.03		6.87	0.14	+0.33	−0.05	+0.80	+0.01
$[Fe@(CrB_6H_6)_2]^{2+}$	2.24	13.92			0.13	+0.34	+0.01	+0.88	+0.03
$Cr@(C_6H_6)_2(D_{5h})$	3.30	2.83	5.40	−0.27					
$Fe@(C_5H_5)_2(D_{5h})$	4.26	7.66	7.14	−0.34					

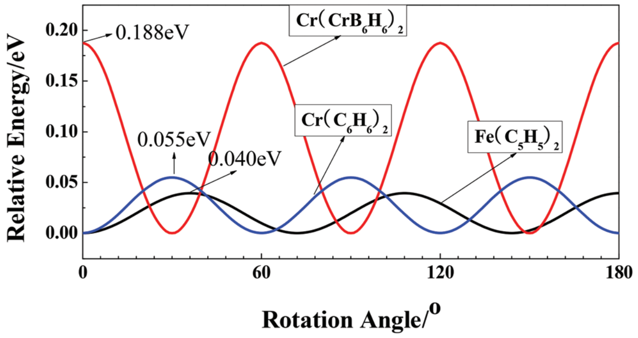

Fig. 2 The energy of $Cr(CrB_6H_6)_2$, $Fe(C_5H_5)_2$ and $Cr(C_6H_6)_2$ in different angles, the most higher energies are labeled in the figure.

zation is always associated with aromaticity, we focus on the aromaticity of those systems. The nucleus-independent chemical shift (NICS) value[72] is an easy and efficient criterion to identify the aromatic nature. A large negative NICS implies the presence of diamagnetic ring currents. Hereby, we calculate NICS values along the *X*-axis of staggered $Cr(CrB_6H_6)_2$, eclipsed $Fe(C_5H_5)_2$ and $Cr(C_6H_6)_2$ in the range of −6.0 to −1.0 Å and 1.0 to 6.0 Å (Fig. 3). In this figure we can see that the variation tendency of the NICS value of $Cr(CrB_6H_6)_2$ is analogous to $Fe(C_5H_5)_2$ and $Cr(C_6H_6)_2$. All of those curves decrease to the most large negative value from 1.0 to 6.0 Å and from −1.0 to −6.0 Å, which is influenced by the center nucleus. Besides, the aromaticity of $Cr(CrB_6H_6)_2$ is lower than that of $Fe(C_5H_5)_2$ and $Cr(C_6H_6)_2$, but the sandwich complex $Cr(CrB_6H_6)_2$ is still aromatic (NICS = −7.11 ppm at $X = 1.5$ Å). The large negative NICS values suggest the strong interaction between the two parallel ligands and the center metal, which means that the sandwich complex is stable. Moreover, the Cr atom in the free ligand shifts by only 0.07 Å after coordination, which indicates that the aromaticity of the ligand is retained in $M(CrB_6H_6)_2$.

3.3. Electronic structures

Why are these sandwich-type structures stable? In ferrocene, the center Fe is in the +2 oxidation state, where the 2 electrons have been transferred to two $[C_5H_5]$s respectively. So the $[C_5H_5]$ has attained the −1 charge state satisfying Huckel's $4n + 2$ rule.[73] Here we give the other answer by NBO analyses.

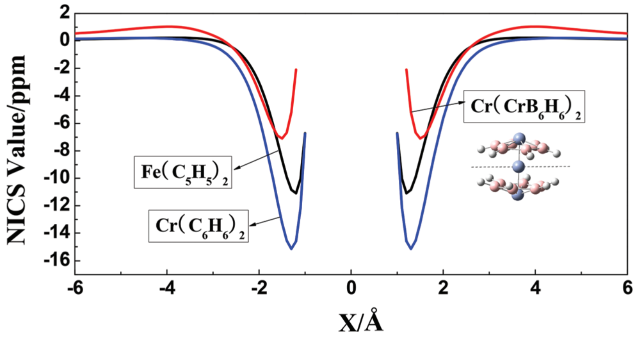

Fig. 3 The NICSxx-scan curves for $Cr(CrB_6H_6)_2$, $Fe(C_5H_5)_2$ and $Cr(C_6H_6)_2$ in the range of −7.0 to −1.0 Å and 1.0 to 7.0 Å in the *X*-axis.

Although the π-MOs of the ligands overlap with the empty orbitals of the center Cr atom, forming the coordination bonds between the CrB_6H_6 ligands and the center Cr, the natural atomic charges of the center Cr atom do not attain negative charges (+0.67 $|e|$). The reason is that the electrons in the 4s orbital of the neutral center Cr have been lost in $Cr(CrB_6H_6)_2$. A similar overlap is found in $[Mn(CrB_6H_6)_2]^+$ and $[Fe(CrB_6H_6)_2]^{2+}$. But the Mn^+ and Fe^{2+} have already lost electrons, so they should be positively charged too. In order to gain insight into the bonding style and delocalized orbital of those clusters, canonical molecular orbital (MO) analysis and the adaptive natural density partitioning (AdNDP) analysis are adopted. AdNDP is a new theoretical tool developed by Boldyrev's group[74,75] for analyzing chemical bonding and it has been successfully applied to organic and inorganic molecules and clusters.[64,66,67,76–80] The size of basis sets does not affect much of the chemical bonding of the compounds, and thus in AdNDP analysis, the 6-31G* and lanl2dz basis sets are employed for nonmetals and transition metals. In the following we pick D_{6d} $Cr(CrB_6H_6)_2$ as examples to discuss their electronic structures.

The $Cr(CrB_6H_6)_2$ has an electronic closed-shell structure, following the 18-electron principle. Similar to $Fe(C_5H_5)_2$, $Cr(C_6H_6)_2$ and $Cr(B_{12})_2$,[66] nine spd–π MOs (Fig. 4) are identified from the canonical MO diagrams. The MO(43) mainly represents the overlaps between the 4s orbital of the center Cr and the π MO of the ligands, whereas the MO(48) reflects the interactions between the $3d_{z^2}$ orbital of the center Cr and the π MO of the ligands. The MO(49) is formed from the $3p_z$ orbital of the center Cr and the π MO of the ligands. The MO(52) and MO(53), and MO(54) and M(55) are double-degenerate orbitals, corresponding to p_x–π and p_y–π, d_{xz}–π and d_{yz}–π, respectively. The HOMOs (MO = 56 and 57) are also double-degenerate orbitals, which result from the π MOs of the ligands and the $3d_{xy}$[1,33] and $3d_{x^2-y^2}$[1,33] of the center Cr.

AdNDP analysis gives more unambiguous details of the chemical bonding of the sandwich. As shown in Fig. 5, AdNDP analysis reveals that there are twelve σ-BH bonds with an

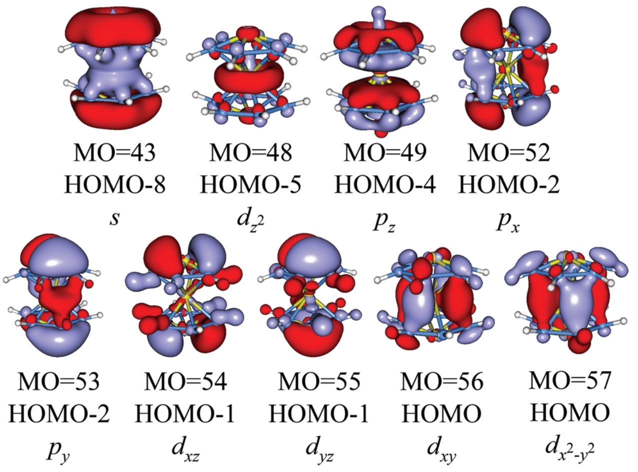

Fig. 4 Partial canonical molecular orbitals of $Cr(CrB_6H_6)_2$.

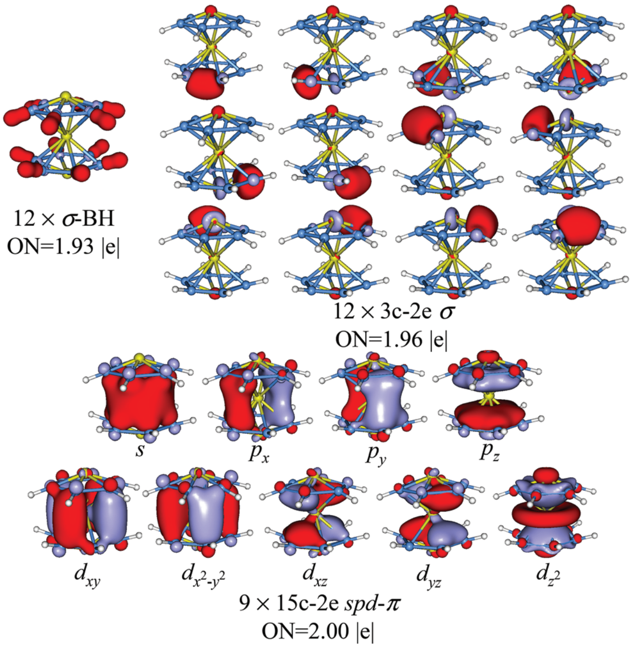

Fig. 5 AdNDP localized bonding patterns of $Cr(CrB_6H_6)_2$.

occupy number (ON) of 1.93 |*e*|, twelve three-center two-electron (3c-2e) σ bonds and nine 15c-2e bonds from the spd–π interaction (ON = 1.96 and 2.00 |*e*|, respectively) in $Cr(CrB_6H_6)_2$. The results show that when the two C_{6v} CrB_6H_6 ligands fasten the Cr atom, only the 7c-2e π bonds of the ligands involve with the spd atomic orbitals of the center Cr, compared to the localized chemical bonding of the ligand.[64] Both the MO analysis and AdNDP analysis illustrate that the spd–π interaction plays an important role in stabilizing the sandwich.

3.4. Discussion

From the analysis above, we know that the bonding style of D_{6d} $Cr(CrB_6H_6)_2$ between the transition metal center and the ligands is nine spd–π interactions. When we replace the Cr with isoelectronic Mn^+ and Fe^{2+}, the bonding styles remain the same (for their partial MOs and AdNDP diagrams see ESI†). With the nuclear charge number increasing, the natural charges of the Cr in the ligands remain almost the same; the positive charges on the transition metal centers are raised remarkably; the negative electrons on the B atoms decrease and even turn to slightly positive charges, which shows that the attraction of the center M with positive charges to the π electrons of the ligands increases and well explains the large binding energy of $[Fe(CrB_6H_6)_2]^{2+}$.

4. Conclusion

In summary, we predict a new class of sandwich-type complexes D_{6d} $M(CrB_6H_6)_2$ ($M = Cr, Mn^+, Fe^{2+}$) by DFT calculations. These sandwich compounds are thermodynamically stable according to their large HOMO–LUMO gap and binding energy, as well as $Fe(C_5H_5)_2$ and $Cr(C_6H_6)_2$, following the 18-electron rule. The NBO analyses show that when the electrons in 4s orbitals of the transition metal center are stripped, the π electrons of the two ligands enter the empty dsp atom orbitals of the center metal at the same time. The double interaction between the two ligands and the metal center is called the spd–π interaction mentioned above, which plays an important role in stabilizing the sandwich. This interaction is confirmed by the MO analysis and AdNDP analysis. The 18 electrons involved in the interaction of the center metal and the two ligands presented nine styles of shape, s, p_x, p_y, p_z, d_{xy}, d_{xz}, d_{yz}, $d_{x^2-y^2}$, and d_{z^2}. The results obtained in this work provide an extension to the traditional concept of sandwich-type complexes, which have a central transition metal atom in the ligand.

Acknowledgements

This work was supported by the National Natural Science Foundation of China (grant no. 21175001, 21273008), by the 211 project of Auhui University. The calculations were carried out at the High-Performance Computing Center of Anhui University. We acknowledge Professor Boldyrev for the AdNDP codes.

Notes and references

1 T. J. Kealy and P. L. Pauson, *Nature*, 1951, **168**, 1039–1040.
2 S. A. Miller, J. A. Tebboth and J. F. Tremaine, *J. Chem. Soc.*, 1952, 632–635.
3 E. O. Fischer and W. Pfab, *Z. Naturforsch. B: Anorg. Chem. Org. Chem. Biochem. Biophys. Biol.*, 1952, **7**, 377–379.
4 G. Wilkinson, M. Rosenblum, M. C. Whiting and R. B. Woodward, *J. Am. Chem. Soc.*, 1952, **74**, 2125–2126.
5 R. B. Woodward, M. Rosenblum and M. C. Whiting, *J. Am. Chem. Soc.*, 1952, **74**, 3458–3459.
6 P. Laszlo and R. Hoffmann, *Angew. Chem., Int. Ed.*, 2000, **39**, 123–124.
7 K. Warren, *Struct. Bonding*, 1976, **27**, 45–159.
8 D. Clark and K. Warren, *Struct. Bonding*, 1980, **39**, 1–41.
9 A. Haaland and J. Nilsson, *Acta Chem., Scand.*, 1968, **22**, 2653–2670.
10 M. B. Hossain and D. Van der Helm, *Inorg. Chem.*, 1978, **17**, 2893–2900.
11 Z. F. Xu, Y. Xie, W. L. Feng and H. F. Schaefer III, *J. Phys. Chem. A*, 2003, **107**, 2716–2729.
12 G. Y. Hong, M. Dolg and L. M. Li, *Int. J. Quantum Chem.*, 2000, **80**, 201–209.
13 R. Muhida, M. M. Rahman, M. Tsuda, T. A. Roman, W. A. Dino, H. Nakanishi and H. Kasai, *J. Phys.: Condens. Matter*, 2004, **16**, S5749–S5753.

14 R. Muhida, H. Setiyanto, M. M. Rahman, W. A. Dino, H. Nakanishi, H. Kasai, K. Fukutani and T. Okano, *Thin Solid Films*, 2006, **509**, 223–226.

15 H. Wang, Y. Xie, R. B. King and H. F. Schaefer, *Eur. J. Inorg. Chem.*, 2008, 3698–3708.

16 A. Togni and R. L. Haltermann, *Metallocenes*, Wiley-VCH, New York, 1998.

17 E. Maslowsky, *Coord. Chem. Rev.*, 2011, **255**, 2746–2763.

18 R. K. Bohn and A. Haaland, *J. Organomet. Chem.*, 1966, **5**, 470–476.

19 S. Masuda, M. Aoyama and Y. Harada, *J. Am. Chem. Soc.*, 1990, **112**, 6445–6446.

20 C. Park and J. Almlof, *J. Chem. Phys.*, 1991, **95**, 1829.

21 W. Klopper and H. P. Luthi, *Chem. Phys. Lett.*, 1996, **262**, 546–552.

22 H. Koch, P. Jorgensen and T. Helgaker, *J. Chem. Phys.*, 1996, **104**, 9528.

23 G. Fronzoni, P. Colavita, M. Stener, G. De Alti and P. Decleva, *J. Phys. Chem. A*, 2001, **105**, 9800–9812.

24 A. Haaland, *Acta Chem., Scand*, 1965, **19**, 41–46.

25 V. M. Rayon and G. Frenking, *Organometallics*, 2003, **22**, 3304–3308.

26 K. Elihn and K. Larsson, *Thin Solid Films*, 2004, **458**, 325–329.

27 G. Frison and A. Sevin, *Internet Electron J. Mol. Des.*, 2004, **3**, 222–232.

28 S. Coriani, A. Haaland, T. Helgaker and P. Jorgensen, *ChemPhysChem*, 2006, **7**, 245–249.

29 G. Zhang, H. Zhang, M. Sun, Y. Liu, X. Pang, X. Yu, B. Liu and Z. Li, *J. Comput. Chem.*, 2007, **28**, 2260–2274.

30 E. Shustorovich and M. Dyatkina, *J. Struct. Chem.*, 1961, **2**, 40–48.

31 D. Den Boer, P. Den Boer and H. Longuet-Higgins, *Mol. Phys.*, 1962, **5**, 387–390.

32 J. Brunvoll, S. Cyvin and L. Schafer, *J. Organomet. Chem.*, 1971, **27**, 69–71.

33 C. Azokpota and C. Pommier, *J. Chem. Thermodyn.*, 1977, **9**, 1121–1125.

34 J. Weber, M. Geoffroy, A. Goursot and E. Penigault, *J. Am. Chem. Soc.*, 1978, **100**, 3995–4003.

35 J. G. Brennan, G. Cooper, J. C. Green, N. Kaltsoyannis, M. A. MacDonald, M. P. Payne, C. M. Redfern and K. H. Sze, *Chem. Phys.*, 1992, **164**, 271–281.

36 L. Phillips and G. R. Dennis, *J. Chem. Soc., Dalton Trans.*, 1995, 1469–1472.

37 C. Elschenbroich, E. Schmidt, R. Gondrum, B. Metz, O. Burghaus, W. Massa and S. Wocadlo, *Organometallics*, 1997, **16**, 4589–4596.

38 R. Sahnoun and C. Mijoule, *J. Phys. Chem. A*, 2001, **105**, 6176–6181.

39 Y. Li and T. Baer, *J. Phys. Chem. A*, 2002, **106**, 9820–9826.

40 I. Gloriozov, A. Y. Vasilkov and Y. A. Ustynyuk, *Russ. J. Phys. Chem. A*, 2006, **80**, 394–405.

41 K. A. Lyssenko, A. A. Korlyukov, D. G. Golovanov, S. Y. Ketkov and M. Y. Antipin, *J. Phys. Chem. A*, 2006, **110**, 6545–6551.

42 S. Y. Ketkov and H. L. Selzle, *Z. Phys. Chem.*, 2007, **221**, 597–607.

43 S. D. Li, J. C. Guo, C. Q. Miao and G. M. Ren, *Angew. Chem., Int. Ed.*, 2005, **44**, 2158–2161.

44 A. D. Garnovskii, A. P. Sadimenko, M. I. Sadimenko and D. A. Garnovskii, *Coord. Chem. Rev.*, 1998, **173**, 31–77.

45 P. V. Schleyer, B. Kiran, D. V. Simion and T. S. Sorensen, *J. Am. Chem. Soc.*, 2000, **122**, 510–513.

46 M. Lein, J. Frunzke, A. Timoshkin and G. Frenking, *Chem. – Eur. J.*, 2001, **7**, 4155–4163.

47 E. Urnezius, W. W. Brennessel, C. J. Cramer, J. E. Ellis and P. V. Schleyer, *Science*, 2002, **295**, 832–834.

48 M. Lein, J. Frunzke and G. Frenking, *Angew. Chem., Int. Ed.*, 2003, **42**, 1303–1306.

49 A. C. Tsipis and A. T. Chaviara, *Inorg. Chem.*, 2004, **43**, 1273–1286.

50 J. C. Guo, W. Z. Yao, Z. Li and S. D. Li, *Sci. China, Ser. B*, 2009, **52**, 566–570.

51 C. Q. Miao, J. C. Guo and S. D. Li, *Sci. China, Ser. B*, 2009, **52**, 900–904.

52 X. Li, A. E. Kuznetsov, H. F. Zhang, A. I. Boldyrev and L. S. Wang, *Science*, 2001, **291**, 859–861.

53 J. M. Mercero, J. M. Matxain and J. M. Ugalde, *Angew. Chem., Int. Ed.*, 2004, **43**, 5485–5488.

54 J. M. Mercero and J. M. Ugalde, *J. Am. Chem. Soc.*, 2004, **126**, 3380–3381.

55 E. Urneúzÿius, W. W. Brennessel, C. J. Cramer, J. E. Ellis and P. R. Schleyer, *Science*, 2002, **95**, 832–834.

56 T. N. Gribanova, A. G. Starikov, R. M. Minyaev, V. I. Minkin, M. R. Siebert and D. J. Tantillo, *Chem. – Eur. J.*, 2010, **16**, 2272–2281.

57 E. Maslowsky, *Coord. Chem. Rev.*, 2011, **255**, 2746–2763.

58 G. N. Srinivas, L. Yu and M. Schwartz, *Organometallics*, 2001, **20**, 5200–5204.

59 v. A. Popov, Z. A. Piazza, W.-L. Li, L.-S. Wang and A. I. Boldyrev, *J. Chem. Phys.*, 2013, **139**, 144307.

60 A. N. Alexandrova, H. J. Zhai, L. S. Wang and A. I. Boldyrev, *Inorg. Chem.*, 2004, **43**, 3552–3554.

61 Q. S. Li and L. F. Gong, *J. Phys. Chem. A*, 2004, **108**, 4322–4325.

62 S. D. Li, C. Q. Miao, J. C. Guo and G. M. Ren, *J. Comput. Chem.*, 2006, **27**, 1858–1865.

63 L. Yang, J. Wang, Y. Ding and C. Sun, *J. Phys. Chem. A*, 2007, **111**, 9122–9129.

64 L. Li, C. Xu, B. Jin and L. Cheng, *J. Chem. Phys.*, 2013, **139**, 174310.

65 J. Tao, J. P. Perdew, V. N. Staroverov and G. E. Scuseria, *Phys. Rev. Lett.*, 2003, **91**, 146401.

66 Y. Yuan and L. Cheng, *J. Chem. Phys.*, 2013, **138**, 024301.

67 L. F. Li and L. J. Cheng, *J. Chem. Phys.*, 2013, **138**, 094312.

68 Y. Yuan and L. J. Cheng, *J. Chem. Phys.*, 2012, **137**, 044308.

69 L. J. Cheng, *J. Chem. Phys.*, 2012, **136**, 104301.

70 M. J. Frisch, G. W. Trucks, H. B. Schlegel, G. E. Scuseria, M. A. Robb, J. R. Cheeseman, G. Scalmani, V. Barone, B. Mennucci, G. A. Petersson, H. Nakatsuji, M. Caricato, X. Li, H. P. Hratchian, A. F. Izmaylov, J. Bloino, G. Zheng, J. L. Sonnenberg, M. Hada, M. Ehara, K. Toyota, R. Fukuda,

J. Hasegawa, M. Ishida, T. Nakajima, Y. Honda, O. Kitao, H. Nakai, T. Vreven, J. A. Montgomery Jr., J. E. Peralta, F. Ogliaro, M. Bearpark, J. J. Heyd, E. Brothers, K. N. Kudin, V. N. Staroverov, R. Kobayashi, J. Normand, K. Raghavachari, A. Rendell, J. C. Burant, S. S. Iyengar, J. Tomasi, M. Cossi, N. Rega, J. M. Millam, M. Klene, J. E. Knox, J. B. Cross, V. Bakken, C. Adamo, J. Jaramillo, R. Gomperts, R. E. Stratmann, O. Yazyev, A. J. Austin, R. Cammi, C. Pomelli, J. W. Ochterski, R. L. Martin, K. Morokuma, V. G. Zakrzewski, G. A. Voth, P. Salvador, J. J. Dannenberg, S. Dapprich, A. D. Daniels, O. Farkas, J. B. Foresman, J. V. Ortiz, J. Cioslowski and D. J. Fox, Gaussian, Inc., Wallingford CT, 2009.

71 H. Chermette, *J. Comput. Chem.*, 1999, **20**, 129.

72 P. v. R. Schleyer, C. Maerker, A. Dransfeld, H. Jiao and N. J. R. van Eikema Hommes, *J. Am. Chem. Soc.*, 1996, **118**, 6317–6318.

73 P. Gütlich, R. Link and A. Trautwein, *Mössbauer spectroscopy and transition metal chemistry*, Springer, Berlin, 1978.

74 D. Y. Zubarev and A. I. Boldyrev, *Phys. Chem. Chem. Phys.*, 2008, **10**, 5207–5217.

75 T. R. Galeev, B. D. Dunnington, J. R. Schmidt and A. I. Boldyrev, *Phys. Chem. Chem. Phys.*, 2013, **15**, 5022–5029.

76 D. Y. Zubarev and A. I. Boldyrev, *J. Org. Chem.*, 2008, **73**, 9251.

77 I. A. Popov and A. I. Boldyrev, *Comput. Theor. Chem.*, 2013, **1004**, 5–11.

78 L. Li, C. Xu and L. Cheng, *Comput. Theor. Chem.*, 2013, **1021**, 144–148.

79 L. J. Cheng, C. D. Ren, X. Z. Zhang and J. L. Yang, *Nanoscale*, 2013, **5**, 1475–1478.

80 L. Cheng and J. Yang, *J. Chem. Phys.*, 2013, **138**, 141101.